TISSUE ENGINEERING: Part C
Volume 20, Number 11, 2014

DOI: 10.1089/ten.tec.2013.0431

Tissue Engineering Chamber Promotes Adipose Tissue Regeneration in Adipose Tissue Engineering Models Through Induced Aseptic Inflammation

Zhangsong Peng, MD,* Ziqing Dong, MD,* Qiang Chang, MD, Weiqing Zhan, MD, Zhaowei Zeng, MD, Shengchang Zhang, MD, and Feng Lu, MD, PhD

Tissue engineering chamber (TEC) makes it possible to generate significant amounts of mature, vascularized, stable, and transferable adipose tissue. However, little is known about the role of the chamber in tissue engineering. Therefore, to investigate the role of inflammatory response and the change in mechanotransduction started by TEC after implantation, we placed a unique TEC model on the surface of the groin fat pads in rats to study the expression of cytokines and tissue development in the TEC. The number of infiltrating cells was counted, and vascular endothelial growth factor (VEGF) and monocyte chemotactic protein-1 (MCP-1) expression levels in the chamber at multiple time points postimplantation were analyzed by enzyme-linked immunosorbent assay. Tissue samples were collected at various time points and labeled for specific cell populations. The result showed that new adipose tissue formed in the chamber at day 60. Also, the expression of MCP-1 and VEGF in the chamber decreased slightly from an early stage as well as the number of the infiltrating cells. A large number of CD34+/perilipin− perivascular cells could be detected at day 30. Also, the CD34+/perilipin+ adipose precursor cell numbers increased sharply by day 45 and then decreased by day 60. CD34−/perilipin+ mature adipocytes were hard to detect in the chamber content at day 30, but their number increased and then peaked at day 60. Ki67-positive cells could be found near blood vessels and their number decreased sharply over time. Masson's trichrome showed that collagen was the dominant component of the chamber content at early stage and was replaced by newly formed small adipocytes over time. Our findings suggested that the TEC implantation could promote the proliferation of adipose precursor cells derived from local adipose tissue, increase angiogenesis, and finally lead to spontaneous adipogenesis by inducing aseptic inflammation and changing local mechanotransduction.

Introduction

One of the major challenges confronting doctors in plastic and reconstructive surgeries is to reconstruct defect areas caused by cancer, trauma, or deformity with large amounts of soft tissue, such as the breast reconstruction after a mastectomy. Potentially, tissue engineering could be applied in all areas of regenerative medical practice.[1] To be more specific, adipose tissue engineering aims to produce new, stable adipose tissues for regenerative and aesthetic medicine.[2–4]

The seed cell, scaffold, and microenvironment were considered as the key factors in tissue engineering. According to this concept, adipose tissue can be reconstructed by combining seed cells with adipogenic potential and biodegradable polymer scaffolds.[5,6] However, by doing so, many researchers failed to maintain the volume of the regenerated adipose tissue over a long implantation period. Mian *et al.* developed a new *in vivo* tissue engineering model for adipose tissue vascularization in 2000, in which a silicone chamber was used to enslave the superficial epigastric vessels.[7] In 2007, Dolderer *et al.* inset a fat flap based on the superficial inferior epigastric vascular pedicle into a hollow plastic chamber implanted subcutaneously in the groin of the rat, which caused significant fat growth.[8] This technique, which is called tissue engineering chamber (TEC), makes it possible to generate significant amounts of mature, vascularized, stable, and transferable adipose tissue, thus introducing a new perspective into adipose tissue engineering.

Based on this technique, subsequent studies suggested that the combination of vascular pedicle, biological scaffolds,

Department of Plastic and Cosmetic Surgery, Nanfang Hospital, Southern Medical University, Guang Zhou, P.R. China.
*These two authors contribute equally and should be cofirst author.

adipogenic growth factors, and adipose-derived stem cells could further promote adipogenesis in TEC.[9–11] However, little is known about the role of the chamber in tissue engineering.

Inflammation is closely related to new adipose tissue formation.[12] An increasing number of studies have demonstrated that cells from adipose lineages (preadipocytes and adipocytes) and macrophages share numerous functional or antigenic properties.[13,14] Preadipocytes and macrophages are similar in their phenotypes, and preadipocytes could efficiently and rapidly convert into macrophages.[15] Monocyte chemotactic protein-1 (MCP-1) is an important chemotactic factor, which is produced predominantly by macrophages, endothelial cells, and preadipocytes, and it would generate proportionally large quantities of new adipose tissue in TEC.[16–20] Without macrophages, there was no tissue growth in the chamber.[21] This strongly suggests a critical role of inflammation in the adipose TEC model.

Angiogenesis and adipogenesis are also closely related in adult neoadipogenesis.[22] A number of angiogenic growth factors acting at specific times in blood vessel development are known to play significant roles in angiogenesis. Vascular endothelial growth factor (VEGF) is one of the key regulators in vascular development.[23] Addition of VEGF to murine TEC could increase early angiogenesis and increase adipose tissue growth at late stage.[24] In addition, both the adipogenesis acceleration and adipogenesis inhibition involve mechanotransduction among cells in the adipose tissue.[25]

Previous studies demonstrated that CD34 is a hallmark of hematopoietic stem cells[26]; it is also expressed in a wide variety of nonhematopoietic cells such as perivascular cells and adipose precursor cells or adipose-derived stem cells (ASCs).[27] Perilipin is a highly phosphorylated adipocyte protein, which locates on the surface of the lipid droplet.[28] The expression of perilipin shows the adipogenesis and maturation from perivascular cells or ASCs into adipocytes.[29] Therefore, combining the two markers of CD34 and perilipin, the CD34+/perilipin− cells, CD34+/perilipin+ cells, and CD34−/perilipin+ cells were identified as perivascular cells, adipose precursor cells (during adipogenic differentiation), and mature adipocytes.

Therefore, we hypothesized that the inflammatory response and the change in mechanotransduction started by TEC implantation could promote the proliferation of adipose precursor cells derived from local adipose tissue, increase angiogenesis, and finally lead to spontaneous adipogenesis. To further investigate this adipogenic process, we placed a unique TEC model on the surface of the groin fat pads in rats to learn the cellular event and the cytokine profiles associated with these cells in different time points after the implantation.

Materials and Methods

Animals, TECs, and surgical techniques

All experiments were performed under the approval of the Nan Fang Hospital Institutional Animal Care and Use Committee. Each hemispheric polycarbonate chamber with an internal diameter of 2 cm and a volume of 2.09 mL was connected to a ring-like Silicon sheet (Fig. 1, left, below), and half of these chambers were connected to ducts (Fig. 1, left, above). All operations were performed on male Sprague Dawley rats (280–300 g, $n=18$) under general anesthesia (10% chloral hydrate administered intraperitoneally at 0.3 mL/100 g body weight). The groins of rats were rendered hair free with an electric shaver, and the skin was then decontaminated with chlorhexidine and alcohol. TECs were inserted bilaterally as described in Vashi *et al.*'s study[30] with modification (Fig. 1, right). First, a transverse incision was made in the groin to reveal the bilateral groin fat pad, which was then anchored to the adjacent muscle fascia with a 10/0 nylon suture. In the space created between the skin and the fat pad, a chamber was placed and fixed. Each rat was implanted with two chambers, one in the left groin with the duct and the other one in the right groin without the duct. With respect to the chamber itself, the silicon sheet with a 1-cm-diameter hole in the center creates an open chamber abutting the surrounding epigastric fat pad, thus providing some contact with adipose tissue. After the implantation, rats were sacrificed at 30, 45, and 60 days, respectively ($n=6$ per time point), and the implanted chambers and their contents were harvested.

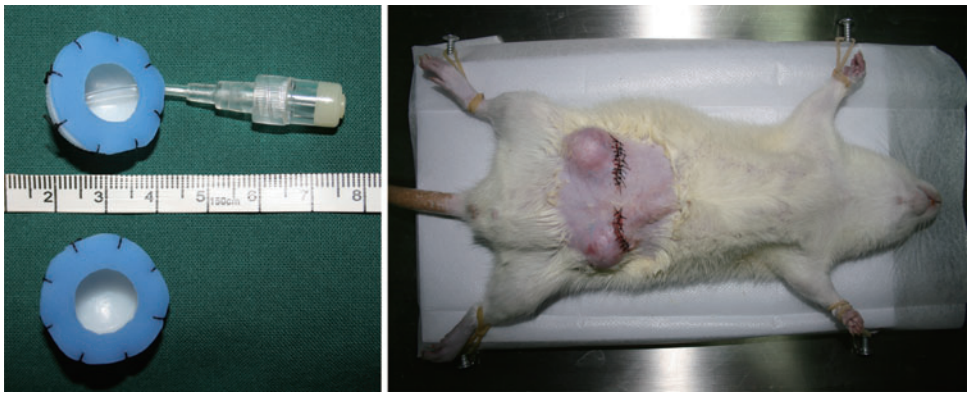

FIG. 1. The rat chamber model. Left: Hemispheric polycarbonate chambers, with an internal diameter of 2 cm and a volume of 2.09 mL, connected to a ring-like Silicon sheet (below) were used, and half of these chambers were connected to ducts (above). Right: The chamber was placed and fixed in the space between the skin and the fat pad. Each rat was implanted with two chambers, one in the left groin with the duct and the other one in the right groin without the duct. Color images available online at www.liebertpub.com/tec

Cell number counting within TEC

At 15, 20, 25, 30, 35, 40, 45, 50, 55, and 60 days postimplantation ($n=6$ per time point), an amount of 0.2 mL fluid was extracted by use of a 1-mL syringe through the duct from each chamber implanted in the left groin. A hemacytometer was used to count the number of cells in the chamber, and eight horizons were assessed. The fluid was also used for further testing.

Characterization of the cytokine expression level of the fluid in TECs

Fluid samples from 10 time points were centrifuged at 3000 rpm for 5 min, and the deposit was removed and stored at −80°C. Serum samples were collected from each rats at the same time point and diluted to 1 mL total volume in phosphate-buffered saline (PBS) as the control group. Quantikine High Sensitivity enzyme-linked immunosorbent assay kits (R&D Systems) were used to assess monocyte MCP-1 and VEGF. An amount of 100 μL diluent was added to each well of an antibody-coated plate before 100 μL of the sample was added. Plates were incubated for 2 h at room temperature and rinsed four times with a wash buffer, and then the buffer was removed and 200 μL of conjugate was added. Next, plates were incubated for another 2 h at room temperature and rinsed four times, and then the buffer was removed and 200 μL of color substrate was added. After an incubation of 30 min in the dark at room temperature, 50 μL of stop solution was added to each well. Plates were read by use of a SpectraMax M5 reader at 450 nm absorbance and contents were analyzed by use of Genesis 2 3.04 (Lifesciences). Values were calculated as nanograms per liter of the original sample volume.

Histological examination and capillary density measuring

Tissues from TECs (experiment group) and adjacent normal adipose tissue (control group) were fixed in 4% paraformaldehyde, dehydrated, and paraffin embedded for hematoxylin and eosin (H&E). Tissue blocks were serially sectioned (5-μm sections) along the longitudinal axis, mounted onto a 3-aminopropyl-triethoxysilane-treated glass slide, then assessed under an Olympus BX51 microscope, and photographed by use of an Olympus DP71 digital camera. Neovascularization was assessed by counting the capillaries in 20 fields of each H&E slide (40× magnification). The counting was performed by two blinded reviewers.

Immunohistochemistry for CD34, perilipin, and Ki67

Immunohistochemistry was used for confirming the cell types at different time points from the samples of both the experimental group and the control group. Two serial sections obtained from each time point (30, 45, and 60 days postimplantation) were examined using the goat anti-rat CD34 antibody (Santa Cruz Biotechnology) and rabbit anti-rat perilipin antibody (Santa Cruz Biotechnology). Also, the rabbit anti-rat Ki67 antibody (Abcam) was used to staining cells for proliferation. Paraffin sections were dewaxed and hydrated before immunohistochemical staining. Slides were washed with PBS and incubated in 3% H_2O_2 for 10 min, after another wash in PBS, and then in a protein block for 30 min by 20% normal goat serum (for CD34) or rabbit serum (for perilipin and Ki67). Then, the sections were incubated with a primary antibody at 4°C overnight. After three wash steps, tissues were incubated with the biotinylated secondary antibody (donkey anti-goat immunoglobulin G [IgG] or goat anti-rabbit IgG; Santa Cruz), diluted 1:200 in PBS for 45 min at room temperature, and subsequently washed with PBS. Following a 30-min incubation with the complex of avidin and biotinylated horseradish peroxidase, the enzyme activity was visualized using 3,3′-diaminobenzidine. Slides were scored by two independent observers using an Olympus BX51 microscope and photographed by use of an Olympus DP71 digital camera.

Collagen quantification

For determination of total collagen, adipose tissue samples obtained at all three time points from the two groups were stained with Masson's trichrome. Briefly, sections were deparaffinized in xylene, rehydrated in graded ethanol, and postfixed in Bouin's fixative for 1 h at 55°C. The nuclei and collagen were sequentially stained with equal volumes of ferric chloride solution and alcoholic hematoxylin and trichrome solution, respectively. The total collagen content was reported as a percentage of the aniline blue staining divided by the total tissue area of the section using ImageJ software.

Statistical analysis

Statistical analyses involved were carried out using SPSS 13.0 (SPSS, Inc.). Results were compared using analysis of variance, with the *post hoc* LSD test as appropriate. $p<0.05$ was considered statistically significant. Data are shown as mean ± standard deviation.

Results

Cell number and cytokine expression

Numerous cells could be detected in the fluid collected from TECs and the number peaked at day 15, then decreased significantly from day 15 to 45 ($p<0.05$), and slightly from day 45 to 60 (Fig. 2, above). The expression of MCP-1 from the chamber decreased slightly from day 15 to 60 (Fig. 2, below, left). The performance of VEGF expression levels from the chamber was similar to MCP-1 (Fig. 2, below, right). Serum VEGF and MCP-1 levels both remained steady at all the time points. However, the serum VEGF and MCP-1 levels were significantly lower than those from the chamber.

Relationship between angiogenesis and adipogenesis in the middle and later stages of adipose tissue development

Inspection of the operation area showed no significant inflammation or tissue necrosis. The TEC content adipose tissue from 30 days was found covered by a capsular layer of well vascularized connective tissue (Fig. 3[1], arrowhead). The samples from 45 days showed a thicker capsular layer, but no significant new adipose formed the chamber (Fig. 3[2], arrowhead). Interestingly, hemispheric new adipose tissue was found in the chamber at day 60, whose

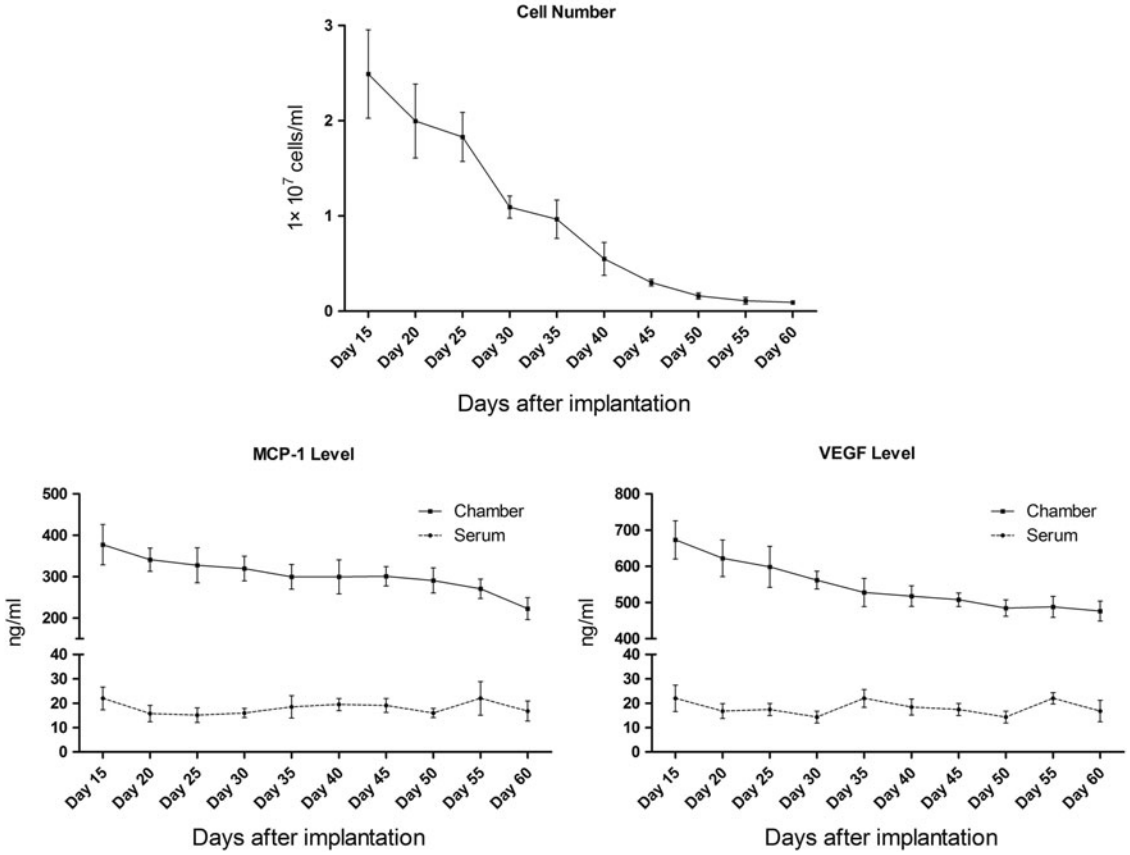

FIG. 2. Cell number of the fluid and the level of monocyte chemotactic protein-1 (MCP-1) and vascular endothelial growth factor (VEGF) (enzyme-linked immunosorbent assay). The cell number of the fluid from tissue engineering chambers (TECs) peaked at day 15, then decreased significantly from day 15 to 45 ($p < 0.05$), and slightly from day 45 to 60. The expression of MCP-1 decreased slightly from day 15 to 60. The changing of the VEGF level was similar to MCP-1. Serum VEGF and MCP-1 levels both remained steady at all the time points and they were significantly lower than those from the chamber.

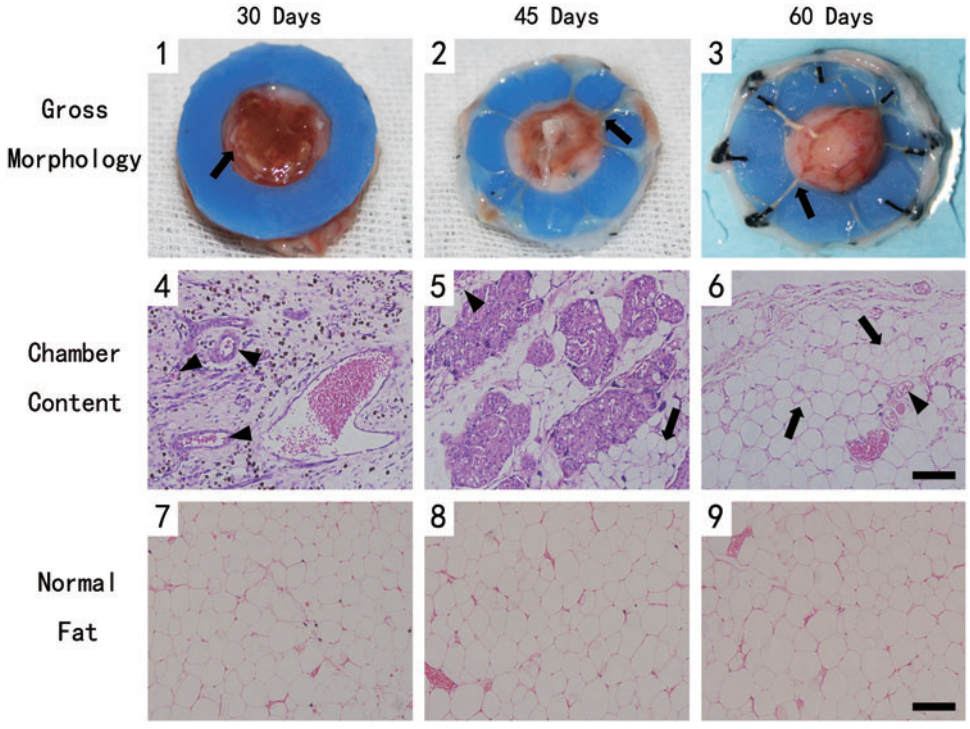

FIG. 3. Tissue formation in the chamber and hematoxylin and eosin (H&E)-stained section at different time points. Scale bar = 100 μm. (1–3) The tissue from 30 days was covered by a well vascularized capsular layer (arrowhead). The capsular became thicker at 45 days. And new adipose tissue formed at day 60. (4) H&E-stained section showed the sample from day 30 contained lots of newly formed vessels (arrowhead), but there was no significant adipogenesis. (5) Small adipocytes (arrow) could be detected from day 45. (6) Vascularized and well-organized adipose tissue (arrow) formed at day 6. (7–9) The adipose tissue from the control group presented a normal phenotype. Color images available online at www.liebertpub.com/tec

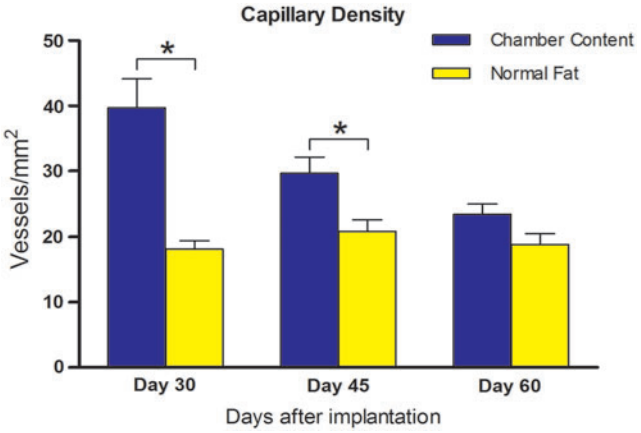

FIG. 4. Capillary density of the newly formed tissue. The capillary density of the TEC content decreased from over time, but it was higher compared with normal adipose tissue at all time points. Statistical analysis was performed among the three time points (*$p < 0.05$). Color images available online at www.liebertpub.com/tec

volume was markedly greater than at earlier time points. A large number of blood vessels could be detected on the surface of the newly formed adipose tissue, and the blood vessels were also connected to the edge of the fat pad (Fig. 3[3], arrowhead).

The histomorphometric analysis demonstrated that the sample from day 30 contained lots of newly formed blood vessels (arrowhead) in the connective tissue, but there was no significant adipogenesis (Fig. 3[4]). Small adipocytes (arrow) could be detected in the connective tissue from day 45 (Fig. 3[5]). By day 60, the TEC content has developed vascularized and well-organized adipose tissue (arrow), which was mature adipose tissue with supporting blood vessels, and the connective tissue decreased (Fig. 3[6]). In addition, the adipose tissue from the control group at all three time points presented a normal phenotype (Fig. 3[7–9]).

Quantification of blood vessels indicated that the capillary density of the TEC content decreased from day 30 (39.7 ± 9.9 vessels/mm^2) and further at later time points (day 45: 29.7 ± 5.6 vessels/mm^2 and day 60: 23.3 ± 3.6 vessels/mm^2). Although the capillary density of the TEC content was higher compared with normal adipose tissue at all three time points, the difference disappeared at day 60 (Fig. 4).

The dynamic change of cell types through different time points

Immunostaining with CD34 and perilipin depicts three different cell populations in the samples from the two groups (Figs. 5 and 6). The CD34+/perilipin− cells (arrowhead) were considered the perivascular cells; double-positive cells with CD34 and perilipin (star) were regarded as adipose precursor cells, and perilipin-positive only cells (arrow) were identified as mature adipocytes.

A large number of CD34+/perilipin− perivascular cells could be detected in the surrounding blood vessels at day 30 after the implantation, but their number decreased over time. By quantification, the cell density of the TEC content was much higher compared with normal adipose tissue at day 30 and 45. However, no differences were noted at day 60 between the two groups (Fig. 7, left). At day 30, only a few CD34+/perilipin+ adipose precursor cells were detected in the tissue, but their number increased sharply by day 45 and then decreased by day 60. In addition, most of the double-positive cells located in the connective tissue surrounding blood vessels, and the cell number of the TEC group at all the time points was significantly higher (Fig. 7, middle).

As to mature adipocytes, the CD34-/perilipin+ cells were hard to detect in chamber content at day 30, but their number increased by day 45, then peaked at day 60, which was even higher, although not significantly, than in normal adipose tissue. The cell shape of these newly formed adipocytes was smaller than normal adipocytes. This explained why their number was a little higher (Fig. 7, right).

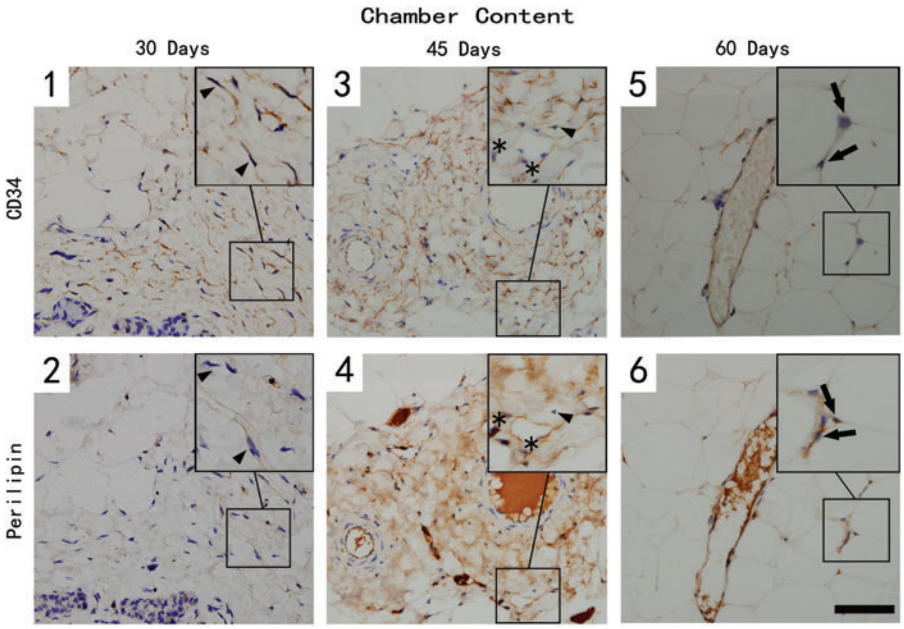

FIG. 5. CD34- and perilipin-stained section of the chamber tissue at different time points. Scale bar = 30 μm. A large number of CD34+/perilipin− (arrowhead) perivascular cells could be detected surrounding blood vessels at day 30 (1 & 2), but their number decreased over time. Only a few CD34+/perilipin+ (star) adipose precursor cells were detected in the tissue, but their number increased sharply by day 45 (3 & 4), then decreased by day 60. CD34−/perilipin+ mature adipocytes (arrow) could be detected in late time point (5 & 6). Color images available online at www.liebertpub.com/tec

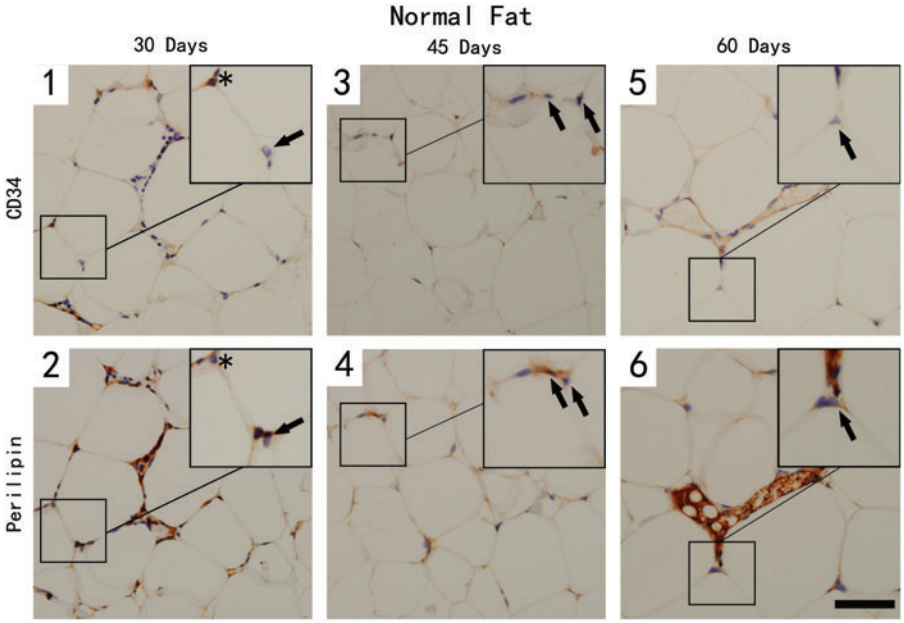

FIG. 6. CD34- and perilipin-stained section of the normal adipose tissue at different time points. Scale bar = 30 μm. CD34 + / perilipin − cells (perivascular cells) and CD34 + /perilipin + (asterisk, adipose precursor cells) were hardly detected in normal adipose tissue at all time points. CD34-/ perilipin + mature adipocytes (arrow) could be detected at all time points. (1–6) The adipose tissue from the control group at three time points. Color images available online at www.liebertpub.com/tec

Cellular proliferation of the TEC content

The proliferation rates of cells in the TEC content and normal adipose tissue were assessed by nuclear staining of Ki67. Interestingly, most Ki67-positive cells (arrowhead) located near blood vessels (star), which was very similar to the distribution of CD34 + /perilipin − perivascular cells (Fig. 8[1–3]). However, few Ki67-positive cells could be found in normal adipose tissue (Fig. 8[4–6]). By quantification, the Ki67-positive cell percentage of the experimental group was significantly higher at all the time points, although it decreased sharply during early stage (Fig. 9).

Collagen staining in adipose tissue

To better demonstrate the extracellular matrix (ECM) growth in the tissue, adipose tissue harvested from both groups was stained with Masson's trichrome, which demonstrated the areas of collagen (blue) staining (Fig. 10A). At day 30, organized collagens and blood vessels were the dominant components of the tissue from TEC (Fig. 10A[1]), then the collagens were gradually replaced by newly formed small adipocytes by day 45 (Fig. 10A[2]). Although the tissue structure of the TEC content was similar to that of the normal adipose tissue at day 60, quantification showed that the TEC group still had a higher collagen content (Fig. 10B).

Discussion

Many studies on adipose tissue engineering have shown that using TEC could produce large volumes of adipose tissue *in vivo*. However, with respect to its mechanism, most of these studies focused on the scaffold material and exogenous growth factors used in the TEC model. After the chamber transplantation, local tissue reacts with continuous inflammation, immune cell infiltration, and ECM reassembly, which is similar to the wound healing process. Moreover, a lot of evidence identified that inflammation and adipogenesis are closely interrelated.[31,32] In this study, we placed the unique polycarbonate TEC model on the surface of rat groin fat pads, and tried to investigate the process of adipose tissue formation and ECM reassembly in TEC in response to the aseptic inflammation through the middle stage and the later stage.

When TEC was implanted *in vivo*, the irritating exogenous materials as well as trauma would cause a local tissue reaction of secreting a large amount of inflammatory factors such as MCP-1, interleukin (IL)-1β, and IL-6.[33] Interestingly, these infiltrated monocytes/macrophages also released inflammatory factors, which provide a signal for more macrophages to enter the TEC. At the beginning of this inflammatory process, monocytes/macrophages could infiltrate into the TEC as early as 12 h postimplantation, with the increase of MCP-1.[34] These cytokines also attract precursor

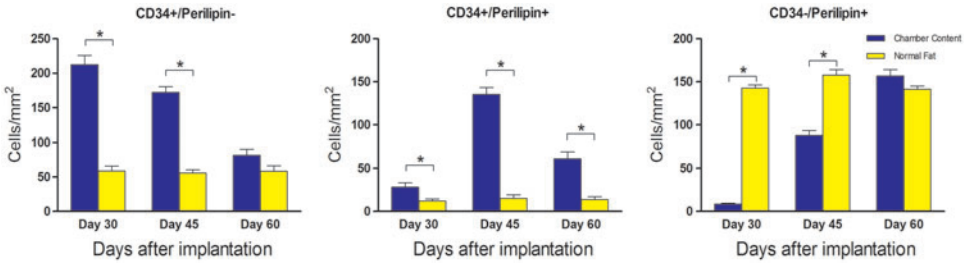

FIG. 7. The cell density of CD34 + /perilipin −, CD34 + /perilipin +, and CD34 − /perilipin + cells. Analysis was performed among the three time points (*$p < 0.05$). Color images available online at www.liebertpub.com/tec

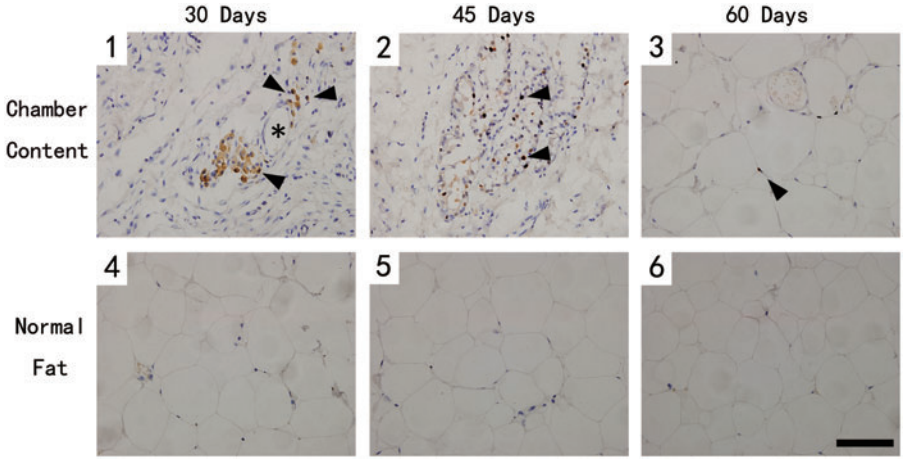

FIG. 8. Ki67-stained section of the samples at different time points. Scale bar = 100 μm. Most Ki67-positive cells (arrowhead) located near blood vessels (star) in chamber tissue. And few Ki67-positive cells could be found in normal adipose tissue. (1–3) The adipose tissue from the experimental group at three time points. (4–6) The adipose tissue from the control group at three time points. Color images available online at www.liebertpub.com/tec

cells such as mesenchymal stem cells (MSCs) into the chamber for tissue repairing.[35] Thus, we propose that the cells we detected in the TEC are mainly monocytes/macrophages from blood circulation and MSCs from local tissue.

Premaratne *et al.* demonstrated that using MSCs could reduce the number of inflammatory factors such as tumor necrosis factor-α, IL-6 in chronic ischemic myocardium.[36] Donizetti-Oliveira *et al.* reported that the adipose tissue MSC treatment prevents renal disease mainly because of the inflammatory response it triggered, which increases the expression of anti-inflammatory factors IL-4 and IL-10.[37] In our study, the MCP-1 level decreased from day 15 after implantation to day 60. This decrease of MCP-1 at the later stage may be due to the immunoregulatory function of MSCs.[38] In addition, both MSCs and macrophages could secrete angiogenic factors such as VEGF and basic fibroblast growth factor.[39–41] The high level of VEGF in the TEC at the early stage after implantation could promote the angiogenic process, and as the angiogenesis gradually completed, the secretion of VEGF decreased. Taken together, we suggest that the high levels of MCP-1 and VEGF in the early and middle stage after implantation enhanced the angiogenesis in the TEC; meanwhile, they also promoted the MSC migration, which became the cellular basis for further adipogenesis.

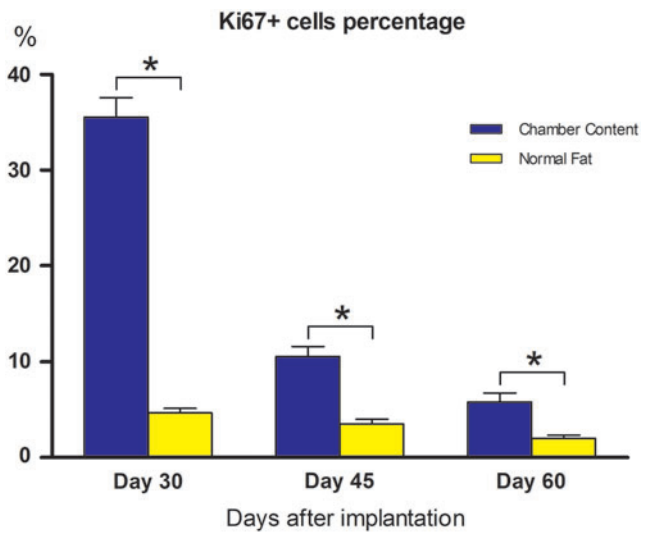

FIG. 9. Ki67+ cell percentage at different time points. Ki67-positive cell percentage of the experimental group was significantly higher at all the time points, although it decreased sharply over time. Analysis was performed among the three time points (*$p < 0.05$). Color images available online at www.liebertpub.com/tec

In our study, a mass of blood vessels developed in the sample of 30 days postimplantation, with a lot of CD34+/perilipin− perivascular cells distributing around the vessels. The Ki67 immunostaining demonstrated that these cells have a high proliferative rate. As perilipin is a highly phosphorylated adipocyte protein that locates on the surface of the lipid droplet,[28] few CD34+/perilipin+ adipose precursor cells or CD34−/perilipin+ mature adipocytes were detected in the tissue. The majority of the CD34+ perivascular cells in the adipose tissue localized in the blood vessels. Their staining was different from that of CD31, in that, CD34+ cells are visible in the adventitia of all blood vessels.[42] Our data also indicated that CD34+ cells in the adipose tissue are more proliferative, while CD34− cells possess greater plasticity.[43] Moreover, activin-A, an adipogenic differentiation inhibitor to adipose precursor cells, however, increases the proliferation of adipose precursor cells.[44] Although a recent study suggested that MCP-1 produced by macrophages can induce adipogenesis through MCP-1-induced protein *in vitro*,[45] our result demonstrated that angiogenesis is the main pathological feature of the newly formed tissue in the TEC in the early and middle stage, and the highly proliferative CD34+/perilipin− perivascular cells would be the key cells for further adipogenic processes.

In the middle and later stages (45 days after implantation), our result showed a decrease in the number of CD34+/perilipin− perivascular cells. Interestingly, the number of CD34+/perilipin+ adipose precursor cells and CD34−/perilipin+ mature adipocytes increased. There is growing evidence that the development of adipose tissue is strongly associated with substantial modulation of the adipose tissue structure, involving adipogenesis, angiogenesis, and extracellular matrix remodeling.[46,47] To supply growing adipose tissue with nutrients and oxygen, the vasculature responds by increasing the number and/or the size of blood vessels, which is the reason why the development of adipose tissue is tightly associated with angiogenesis.[48] When the tissue had finely vascularized, some of the perivascular cells became perilipin

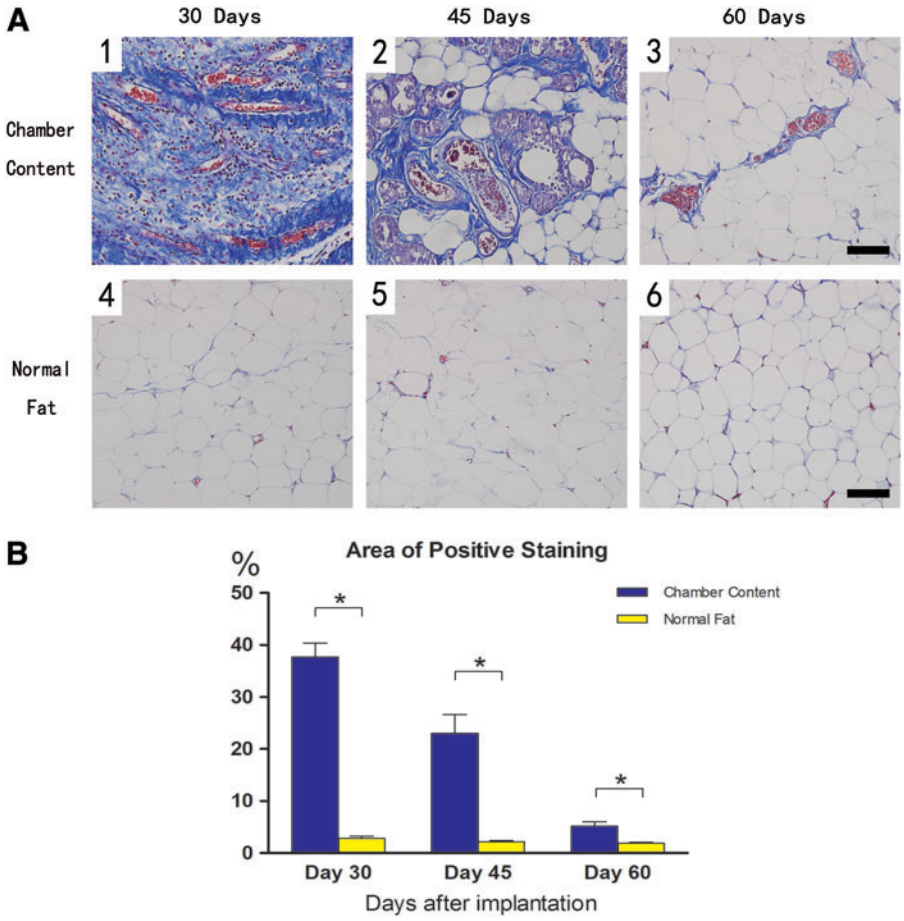

FIG. 10. The Masson's trichrome stain at different time points. Scale bar = 100 μm. **(A)** At day 30 (1), organized collagens and blood vessels were the dominant components of the tissue from TEC. Collagens were then replaced by newly formed small adipocytes by day 45 (2). The TEC tissue structure became similar to that of the normal adipose tissue at day 60 (3). The adipose tissue from the control group (4–6). **(B)** Quantification showed that the experimental group had a higher collagen content at all the time points. Analysis was performed among the three time points ($*p < 0.05$). Color images available online at www.liebertpub.com/tec

positive and ki67 negative, which suggests that these perivascular cells stopped proliferating and differentiated to adipose precursor cells and then to mature adipocytes. Then, adipogenesis began to play a major role in further adipose tissue regeneration. At day 60, the late stage after implantation, the structure of the newly formed adipose tissue was well organized. The major cell component in the tissue was mature adipocytes, which means that the neoadipogenesis in the TEC was nearly completed.

In adipose tissue, mature adipocytes and stromal cells live in a three-dimensional network constructed by ECM proteins. The function of adipose tissue is regulated by cells and a variety of ECM proteins through physiological interactions.[49] Notably, excessive ECM deposition in adipose

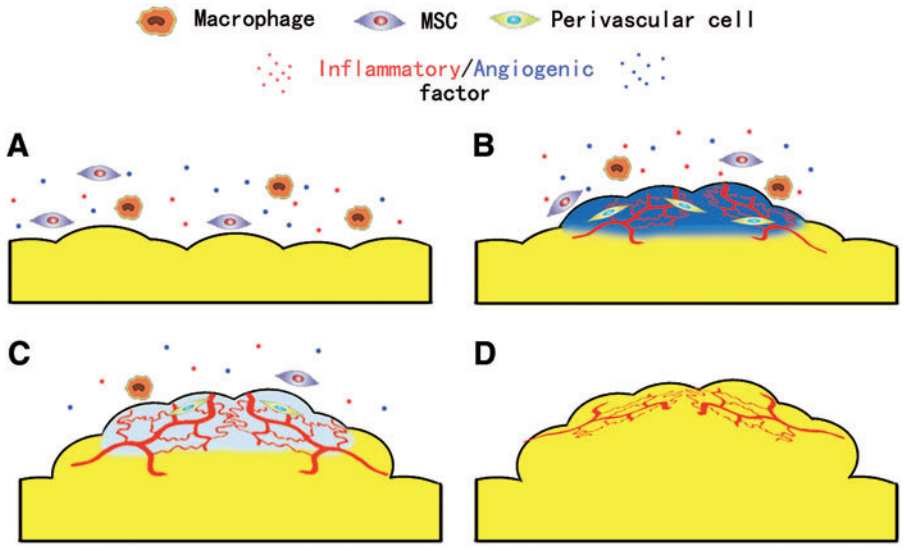

FIG. 11. The neoadipogenesis within the TEC. **(A)** In the inflammation stage, the macrophage/mesenchymal stem cell (MSC) infiltration as well as inflammatory/angiogenic factor release. **(B)** The angiogenesis stage inflammation remarkably enhanced the angiogenesis and the extracellular matrix (ECM) expansion as well as the proliferation of perivascular cells. **(C)** In the adipogenesis stage, perivascular cells turned into adipose precursor cells and adipogenic differentiation began. **(D)** Finally, in the maturation stage, after the expansion of newly formed adipocyte tissue and ECM remodeling, the neoadipogenesis completed. Color images available online at www.liebertpub.com/tec

tissue was observed along with inflammatory tissue damage, which is characterized by the infiltration of neutrophils, lymphocytes, and macrophages. Thus, fibrotic tissue damage is perceived by many as a process secondary to tissue inflammation in obesity in recent years.[50–52] After tissue injury, fibrinogens leaking from ligated blood vessels form fibrin clots, which fill up spaces in the wound.[53,54] Moreover, many studies have reported that fibrin enhances the angiogenesis of wound healing *in vitro* and *in vivo*.[55,56] We found ECM hyperplasia in the early stage after implantation as well as a high level of MCP-1, which indicated the inflammatory response caused by exogenous materials and the expansion of inflammation caused by the operation. This expansion promoted the angiogenesis of local tissue then. With the adipose tissue remolding in the later time point, its histological structure becomes normal gradually.

Considered together, in our study, we observed that the adipose tissue regeneration in TEC could be divided into four stages, the inflammation stage (0–15 day), the angiogenesis stage (15–30 day), the adipogenesis stage (30–45 day), and the maturation stage (45–60 day). In the inflammation stage, the implantation of chamber and surgery stimulated macrophages/MSC infiltration as well as inflammatory/angiogenic factor release (Fig. 11A). Then, the inflammatory reaction remarkably enhanced the angiogenesis and the ECM expansion of the TEC content and the proliferation of perivascular cells (Fig. 11B). In the adipogenesis stage, with adequate blood supply, perivascular cells turned into adipose precursor cells and adipogenic differentiation began (Fig. 11C). Finally, in the maturation stage, after the expansion of newly formed adipocyte tissue and ECM remodeling, the adipose tissue regeneration completed (Fig. 11D).

Conclusion

In this study, we adopted a specially designed TEC model to investigate the adipocyte tissue regeneration mode in the TEC. Our findings suggested that the TEC implantation could promote the proliferation of adipose precursor cells derived from local adipose tissue, increase angiogenesis, and finally lead to spontaneous adipogenesis by inducing aseptic inflammation and changing local mechanotransduction. The new information mentioned above may provide a new idea for studies on obesity, metabolism syndrome, even diabetes, and we can also use it to guide adipose tissue engineering researches for reconstructive purposes.

Acknowledgments

This work was supported by the National Nature Science Foundation of China 81171834, 81071589.

Disclosure Statement

All the authors (Z.P., Z.D., Q.C., W.Z., Z.Z., S.Z., and F.L.) report grants from the National Nature Science Foundation of China 81171834, grants from the National Nature Science Foundation of China 81071589, during the conduct of the study.

References

1. Langer, R.V.J. Tissue engineering. Science **260,** 920, 1993.
2. Casadei, A., Epis, R., Ferroni, L., Tocco, I., Gardin, C., Bressan, E., Sivolella, S., Vindigni, V., Pinton, P., Mucci, G., and Zavan, B. Adipose tissue regeneration: a state of the art. J Biomed Biotechnol **2012, 462543,** 2012.
3. Choi, J.H., Gimble, J.M., Lee, K., Marra, K.G., Rubin, J.P., Yoo, J.J., Vunjak-Novakovic, G., and Kaplan, D.L. Adipose tissue engineering for soft tissue regeneration. Tissue Eng Part B Rev **16,** 413, 2010.
4. Sterodimas, A., De Faria, J., Correa, W.E., and Pitanguy, I. Tissue engineering in plastic surgery: an up-to-date review of the current literature. Ann Plast Surg **62,** 97, 2009.
5. von Heimburg, D., Zachariah, S., Heschel, I., Kuhling, H., Schoof, H., Hafemann, B., and Pallua, N. Human preadipocytes seeded on freeze-dried collagen scaffolds investigated *in vitro* and *in vivo*. Biomaterials **22,** 429, 2001.
6. Patrick, C.J., Zheng, B., Johnston, C., and Reece, G.P. Long-term implantation of preadipocyte-seeded PLGA scaffolds. Tissue Eng **8,** 283, 2002.
7. Mian, R., Morrison, W.A., Hurley, J.V., Penington, A.J., Romeo, R., Tanaka, Y., and Knight, K.R. Formation of new tissue from an arteriovenous loop in the absence of added extracellular matrix. Tissue Eng **6,** 595, 2000.
8. Dolderer, J.H., Abberton, K.M., Thompson, E.W., Slavin, J.L., Stevens, G.W., Penington, A.J., and Morrison, W.A. Spontaneous large volume adipose tissue generation from a vascularized pedicled fat flap inside a chamber space. Tissue Eng **13,** 673, 2007.
9. Lokmic, Z., Stillaert, F., Morrison, W.A., Thompson, E.W., and Mitchell, G.M. An arteriovenous loop in a protected space generates a permanent, highly vascular, tissue-engineered construct. Faseb J **21,** 511, 2007.
10. Yuksel, E., Weinfeld, A.B., Cleek, R., Wamsley, S., Jensen, J., Boutros, S., Waugh, J.M., Shenaq, S.M., and Spira, M. Increased free fat-graft survival with the long-term, local delivery of insulin, insulin-like growth factor-I, and basic fibroblast growth factor by PLGA/PEG microspheres. Plast Reconstr Surg **105,** 1712, 2000.
11. Yuksel, E., Weinfeld, A.B., Cleek, R., Waugh, J.M., Jensen, J., Boutros, S., Shenaq, S.M., and Spira, M. *De novo* adipose tissue generation through long-term, local delivery of insulin and insulin-like growth factor-1 by PLGA/PEG microspheres in an *in vivo* rat model: a novel concept and capability. Plast Reconstr Surg **105,** 1721, 2000.
12. Thomas, G.P., Hemmrich, K., Abberton, K.M., McCombe, D., Penington, A.J., Thompson, E.W., and Morrison, W.A. Zymosan-induced inflammation stimulates neo-adipogenesis. Int J Obes (Lond) **32,** 239, 2008.
13. Schaffler, A., Muller-Ladner, U., Scholmerich, J., and Buchler, C. Role of adipose tissue as an inflammatory organ in human diseases. Endocr Rev **27,** 449, 2006.
14. Gustafson, B., Gogg, S., Hedjazifar, S., Jenndahl, L., Hammarstedt, A., and Smith, U. Inflammation and impaired adipogenesis in hypertrophic obesity in man. Am J Physiol Endocrinol Metab **297,** 999, 2009.
15. Charriere, G., Cousin, B., Arnaud, E., Andre, M., Bacou, F., Penicaud, L., and Casteilla, L. Preadipocyte conversion to macrophage. Evidence of plasticity. J Biol Chem **278,** 9850, 2003.
16. Hemmrich, K., Thomas, G.P., Abberton, K.M., Thompson, E.W., Rophael, J.A., Penington, A.J., and Morrison, W.A. Monocyte chemoattractant protein-1 and nitric oxide promote adipogenesis in a model that mimics obesity. Obesity (Silver Spring) **15,** 2951, 2007.

17. Matsushima, K., Larsen, C.G., DuBois, G.C., and Oppenheim, J.J. Purification and characterization of a novel monocyte chemotactic and activating factor produced by a human myelomonocytic cell line. J Exp Med **169,** 1485, 1989.
18. Menghini, R., Marchetti, V., Cardellini, M., Hribal, M.L., Mauriello, A., Lauro, D., Sbraccia, P., Lauro, R., and Federici, M. Phosphorylation of GATA2 by Akt increases adipose tissue differentiation and reduces adipose tissue-related inflammation: a novel pathway linking obesity to atherosclerosis. Circulation **111,** 1946, 2005.
19. Rollins, B.J. Chemokines. Blood **90,** 909, 1997.
20. Yoshimura, T., Robinson, E.A., Tanaka, S., Appella, E., Kuratsu, J., and Leonard, E.J. Purification and amino acid analysis of two human glioma-derived monocyte chemoattractants. J Exp Med **169,** 1449, 1989.
21. Debels, H., Galea, L., Han, X.L., Palmer, J., van Rooijen, N., Morrison, W., and Abberton, K. Macrophages play a key role in angiogenesis and adipogenesis in a mouse tissue engineering model. Tissue Eng Part A **19,** 2615, 2013.
22. Fukumura, D., Ushiyama, A., Duda, D.G., Xu, L., Tam, J., Krishna, V., Chatterjee, K., Garkavtsev, I., and Jain, R.K. Paracrine regulation of angiogenesis and adipocyte differentiation during *in vivo* adipogenesis. Circ Res **93,** e88, 2003.
23. Carmeliet, P., and Jain, R.K. Molecular mechanisms and clinical applications of angiogenesis. Nature **473,** 298, 2011.
24. Rophael, J.A., Craft, R.O., Palmer, J.A., Hussey, A.J., Thomas, G.P., Morrison, W.A., Penington, A.J., and Mitchell, G.M. Angiogenic growth factor synergism in a murine tissue engineering model of angiogenesis and adipogenesis. Am J Pathol **171,** 2048, 2007.
25. Shoham, N., and Gefen, A. Mechanotransduction in adipocytes. J Biomech **45,** 1, 2012.
26. Lange, C., Li, Z., Fang, L., Baum, C., and Fehse, B. CD34 modulates the trafficking behavior of hematopoietic cells *in vivo*. Stem Cells Dev **16,** 297, 2007.
27. Eto, H., Ishimine, H., Kinoshita, K., Watanabe-Susaki, K., Kato, H., Doi, K., Kuno, S., Kurisaki, A., and Yoshimura, K. Characterization of human adipose tissue-resident hematopoietic cell populations reveals a novel macrophage subpopulation with CD34 expression and mesenchymal multipotency. Stem Cells Dev **22,** 985, 2013.
28. Greenberg, A.S., Egan, J.J., Wek, S.A., Garty, N.B., Blanchette-Mackie, E.J., and Londos, C. Perilipin, a major hormonally regulated adipocyte-specific phosphoprotein associated with the periphery of lipid storage droplets. J Biol Chem **266,** 11341, 1991.
29. Brasaemle, D.L., Barber, T., Wolins, N.E., Serrero, G., Blanchette-Mackie, E.J., and Londos, C. Adipose differentiation-related protein is an ubiquitously expressed lipid storage droplet-associated protein. J Lipid Res **38,** 2249, 1997.
30. Vashi, A.V., Abberton, K.M., Thomas, G.P., Morrison, W.A., O'Connor, A.J., Cooper-White, J.J., and Thompson, E.W. Adipose tissue engineering based on the controlled release of fibroblast growth factor-2 in a collagen matrix. Tissue Eng **12,** 3035, 2006.
31. Spencer, M., Yao-Borengasser, A., Unal, R., Rasouli, N., Gurley, C.M., Zhu, B., Peterson, C.A., and Kern, P.A. Adipose tissue macrophages in insulin-resistant subjects are associated with collagen VI and fibrosis and demonstrate alternative activation. Am J Physiol Endocrinol Metab **299,** 1016, 2010.
32. Pasarica, M., Sereda, O.R., Redman, L.M., Albarado, D.C., Hymel, D.T., Roan, L.E., Rood, J.C., Burk, D.H., and Smith, S.R. Reduced adipose tissue oxygenation in human obesity: evidence for rarefaction, macrophage chemotaxis, and inflammation without an angiogenic response. Diabetes **58,** 718, 2009.
33. Krysko, D.V., Denecker, G., Festjens, N., Gabriels, S., Parthoens, E., D'Herde, K., and Vandenabeele, P. Macrophages use different internalization mechanisms to clear apoptotic and necrotic cells. Cell Death Differ **13,** 2011, 2006.
34. Lilja, H.E., Morrison, W.A., Han, X.L., Palmer, J., Taylor, C., Tee, R., Moller, A., Thompson, E.W., and Abberton, K.M. An adipoinductive role of inflammation in adipose tissue engineering: key factors in the early development of engineered soft tissues. Stem Cells Dev **22,** 1602, 2013.
35. Patel, D.M., Shah, J., and Srivastava, A.S. Therapeutic potential of mesenchymal stem cells in regenerative medicine. Stem Cells Int **2013,** 496218, 2013.
36. Premaratne, G.U., Ma, L.P., Fujita, M., Lin, X., Bollano, E., and Fu, M. Stromal vascular fraction transplantation as an alternative therapy for ischemic heart failure: anti-inflammatory role. J Cardiothorac Surg **6,** 43, 2011.
37. Donizetti-Oliveira, C., Semedo, P., Burgos-Silva, M., Cenedeze, M.A., Malheiros, D.M., Reis, M.A., Pacheco-Silva, A., and Camara, N.O. Adipose tissue-derived stem cell treatment prevents renal disease progression. Cell Transplant **21,** 1727, 2012.
38. Shi, Y., Su, J., Roberts, A.I., Shou, P., Rabson, A.B., and Ren, G. How mesenchymal stem cells interact with tissue immune responses. Trends Immunol **33,** 136, 2012.
39. Kawanishi, N., Yano, H., Yokogawa, Y., and Suzuki, K. Exercise training inhibits inflammation in adipose tissue via both suppression of macrophage infiltration and acceleration of phenotypic switching from M1 to M2 macrophages in high-fat-diet-induced obese mice. Exerc Immunol Rev **16,** 105, 2010.
40. Mosser, D.M. The many faces of macrophage activation. J Leukoc Biol **73,** 209, 2003.
41. Pollard, J.W. Tumour-educated macrophages promote tumour progression and metastasis. Nat Rev Cancer **4,** 71, 2004.
42. Lin, G., Garcia, M., Ning, H., Banie, L., Guo, Y.L., Lue, T.F., and Lin, C.S. Defining stem and progenitor cells within adipose tissue. Stem Cells Dev **17,** 1053, 2008.
43. Suga, H., Matsumoto, D., Eto, H., Inoue, K., Aoi, N., Kato, H., Araki, J., and Yoshimura, K. Functional implications of CD34 expression in human adipose-derived stem/progenitor cells. Stem Cells Dev **18,** 1201, 2009.
44. Zaragosi, L.E., Wdziekonski, B., Villageois, P., Keophiphath, M., Maumus, M., Tchkonia, T., Bourlier, V., Mohsen-Kanson, T., Ladoux, A., Elabd, C., Scheideler, M., Trajanoski, Z., Takashima, Y., Amri, E.Z., Lacasa, D., Sengenes, C., Ailhaud, G., Clement, K., Bouloumie, A., Kirkland, J.L., and Dani, C. Activin a plays a critical role in proliferation and differentiation of human adipose progenitors. Diabetes **59,** 2513, 2010.
45. Younce, C.W., Azfer, A., and Kolattukudy, P.E. MCP-1 (monocyte chemotactic protein-1)-induced protein, a recently identified zinc finger protein, induces adipogenesis in 3T3-L1 pre-adipocytes without peroxisome proliferator-activated receptor gamma. J Biol Chem **284,** 27620, 2009.
46. Cao, Y. Adipose tissue angiogenesis as a therapeutic target for obesity and metabolic diseases. Nat Rev Drug Discov **9,** 107, 2010.

47. Lijnen, H.R. Angiogenesis and obesity. Cardiovasc Res **78,** 286, 2008.
48. Scroyen, I., Hemmeryckx, B., and Lijnen, H.R. From mice to men: mouse models in obesity research: what can we learn? Thromb Haemost **110,** 634, 2013.
49. Chun, T.H. Peri-adipocyte ECM remodeling in obesity and adipose tissue fibrosis. Adipocyte **1,** 89, 2012.
50. Schenk, S., Saberi, M., and Olefsky, J.M. Insulin sensitivity: modulation by nutrients and inflammation. J Clin Invest **118,** 2992, 2008.
51. Lumeng, C.N., and Saltiel, A.R. Inflammatory links between obesity and metabolic disease. J Clin Invest **121,** 2111, 2011.
52. Gregor, M.F., and Hotamisligil, G.S. Inflammatory mechanisms in obesity. Annu Rev Immunol **29,** 415, 2011.
53. Clark, R.A., Nielsen, L.D., Welch, M.P., and McPherson, J.M. Collagen matrices attenuate the collagen-synthetic response of cultured fibroblasts to TGF-beta. J Cell Sci **108,** 1251, 1995.
54. McClain, S.A., Simon, M., Jones, E., Nandi, A., Gailit, J.O., Tonnesen, M.G., Newman, D., and Clark, R.A. Mesenchymal cell activation is the rate-limiting step of granulation tissue induction. Am J Pathol **149,** 1257, 1996.
55. Takei, A., Tashiro, Y., Nakashima, Y., and Sueishi, K. Effects of fibrin on the angiogenesis *in vitro* of bovine endothelial cells in collagen gel. In Vitro Cell Dev Biol Anim **31,** 467, 1995.
56. Dvorak, H.F., Harvey, V.S., Estrella, P., Brown, L.F., McDonagh, J., and Dvorak, A.M. Fibrin containing gels induce angiogenesis. Implications for tumor stroma generation and wound healing. Lab Invest **57,** 673, 1987.

Address correspondence to:
Feng Lu, MD, PhD
Department of Plastic and Cosmetic Surgery
Nanfang Hospital
Southern Medical University
1838 Guangzhou North Road
Guang Zhou, Guangdong 510515
P.R. China

E-mail: doctorlufeng@hotmail.com

Received: July 16, 2013
Accepted: February 19, 2014
Online Publication Date: March 28, 2014